J|A|C|S
ARTICLES
Published on Web 04/06/2002

Molecular Rulers: New Families of Molecules for Measuring Interfacial Widths

William H. Steel, Fehmi Damkaci, Ryan Nolan,† and Robert A. Walker*

Contribution from the Department of Chemistry and Biochemistry, University of Maryland-College Park, College Park, Maryland 20742

Received October 30, 2001

Abstract: Homologous series of solvatochromic neutral alcohols and ionic sulfates are synthesized and characterized. Each surfactant series consists of hydrophobic, *p*-nitroanisole-based chromophores attached to polar or ionic headgroups by *n*-alkyl spacers. UV absorption measurements show that the optical properties of surfactant chromophores closely track those of the parent chromophore. Interfacial tension measurements are used to calculate surface excess concentrations of ionic surfactants adsorbed to an aqueous−cyclohexane interface. With a hydrophobic chromophore, a hydrophilic headgroup, and a variable-length, alkyl spacer, these surfactants have the potential to function as molecular rulers: probes of molecular-scale variation in solvation forces across condensed-phase interfaces. Changing the separation between the hydrophobic, solvatochromic probe and the hydrophilic headgroup should enable different members of a homologous series to span different interfacial widths, thus exposing the chromophore to different chemical environments. This idea is explored by using surface-specific, nonlinear optical spectroscopy. Resonant second harmonic spectra of *p*-nitroanisole and the surfactant product **4a** adsorbed to an aqueous−cyclohexane interface show the surfactant spectrum blue-shifted 9 nm relative to the spectrum of adsorbed *p*-nitroanisole. On the basis of chromophore solvatochromism, these results are consistent with a less polar environment surrounding the surfactant chromophore. Significant differences in interfacial solvation resulting from a ∼5 Å separation between the surfactant headgroup and chromophore support recently proposed models of molecularly sharp, microscopically flat aqueous−alkane interfaces.

Introduction

Common experience shows that oil and water do not mix and that water will wet a hydrophilic substrate but not a hydrophobic substrate. Supporting these observations are numerous experimental and theoretical investigations that demonstrate how surfaces alter the properties of an adjacent solvent from bulk solution limits.[1] These findings appeal to intuition. Boundaries between a solid and a liquid or two immiscible liquids create environments in which an imbalance in forces leads to large changes in long-range solvent structure, density, and polarity.[2]

Less intuitive are the characteristic length scales over which these surface-induced effects extend. Given that surface-mediated solvent properties control the concentration, conformation, and reactivity of adsorbed solute species, determining the width of interfacial regions has the potential to impact significantly models and mechanisms of solution-phase, surface chemistry.[3] Affected phenomena can be as simple as elementary surface reactions whose rates depend sensitively on solvent polarity[4] or as complex as protein recognition at cell membrane surfaces—an event that is exceedingly sensitive to local gradients in pH and ionic strength.[5] Chemical transport across liquid interfaces—the heart of solvent extraction—depends on interfacial solvent viscosity, permittivity, and relaxation rates.[6]

Previous experimental studies of interfacial solvation characterized solvent polarity at the boundaries between weakly associating, immiscible liquids.[7] Here, the term weakly associating refers to two adjacent phases (aqueous and organic) that interact through weak dipole−dipole or dispersion forces. The model of interfacial polarity that emerges from nonlinear optical (NLO) experiments is that of an interface whose dielectric properties reflect a simple, averaged contribution from the two adjacent phases.[2b] While this result may seem surprising

* Address correspondence to this author. E-mail: rw158@umail.umd.edu.
† Materials Research Science and Engineering Center at the University of Maryland, College Park, MD 20742.

(1) (a) Benjamin, I. *Chem. Rev.* **1996**, *96*, 1449−14775. (b) Eisenthal, K. B. *J. Phys. Chem.* **1996**, *100*, 12997−13006. (c) Richmond, G. L. *Annu. Rev. Phys. Chem.* **2001**, *52*, 357−389. (d) Penfold, J.; et al. *J. Chem. Soc., Faraday Trans.* **1997**, *93*, 3899−3917. (e) Lee, S. H.; Rossky, P. J. *J. Chem. Phy.* **1994**, *100*, 3334−3345.
(2) (a) Mitrinovic, D. M.; Schlossman, M. L.; et al. *Phy. Rev. Lett.* **2000**, *85*, 582−585. (b) Wang, H.; Borguet, E.; Eisenthal, K. B. *J. Phys. Chem. A* **1997**, *101*, 713−718. (c) Stanners, C. D.; Shen, Y.-R.; et al. *Chem. Phys. Lett.* **1995**, *232*, 407−413. (d) Zhang, X.; Esenturk, O.; Walker, R. A. *J. Am. Chem. Soc.* **2001**, *123*, 10768−10769. (e) Zhang, X.; Walker, R. A. *Langmuir* **2001**, *17*, 4486-4489. (f) Tikhonov, A. M.; Schlossman, M. L.; et al. *J. Phys. Chem. B* **2000**, *104*, 6336−6339.
(3) Michael, D.; Benjamin, I. *J. Phys. Chem.* **1997**, *107*, 5684−5693 and references therein.
(4) (a) Sola, M.; Duran, M.; et al. *J. Am. Chem. Soc.* **1991**, *113*, 2873−2879. (b) Reichardt, C. *Solvent Effects in Organic Chemistry*; Veralg Chemie: New York, 1979; Chapter 1.
(5) Safran, S. A. *Statistical Thermodynamics of Surfaces, Interfaces, and Membranes*; Pines, D., Ed.; Addison-Wesley Publishing Company: Reading, MA, 1994.
(6) Freiser, H. *Chem. Rev.* **1988**, *88*, 611−616.
(7) (a) Wang H.; Borguet, E.; Eisenthal, K. B. *J. Phys. Chem. B* **1998**, *102*, 4927−4932. (b) Kitamura, N.; Ishizaka, S.; et al. *Anal. Chem.* **1999**, *71*, 3382−3389. (c) Kitamura, N.; Ishizaka, S.; et al. *Anal. Chem.* **2001**, *73*, 2421−2428.

10.1021/ja012457u CCC: $22.00

at first, given the strong anisotropy inherent to interfacial regions, the effect can be understood in terms of a liquid−liquid interface that is both (a) molecularly sharp (properties of one phase converge to those of the other in only a few solvent layers) and (b) microscopically flat (very little thermal roughening on the molecular scale due to capillary wave activity). Such a picture is consistent with simulations describing the interfacial properties between an aqueous solvent and a nonpolar, hydrocarbon solvent.[8]

Other studies, however, suggested that the "average-polarity" model breaks down when the adjacent organic solvent is polar (but aprotic). Specifically, interfacial polarity inferred from fluorescence measurements at polar organic−aqueous interfaces was considerably less than that predicted by averaged contributions from the two adjacent phases. This result could indicate an interface that was either molecularly diffuse or thermally roughened, although simulations predict that a roughened interface should be *more polar* than a molecularly flat boundary.[7c] Further complicating interpretation of the fluorescence results is the fact that the technique is not surface specific, meaning that even experiments carried out under total internal reflection conditions sample up to tens of nanometers into the phase with the lower refractive index. In contrast, nonlinear optical experiments *are* surface specific, with signals originating only within the anisotropic boundary between two isotropic phases.

While these NLO, fluorescence, and molecular dynamics studies of interfacial solvation raise important questions about how interfacial anisotropy influences the local chemical environment *experienced by solutes*, the experiments themselves suffered from several limitations. First, the probes were generally large relative to the size of solvent species in each phase. In some cases, the probes consisted of fused aromatic systems containing up to seven six-membered rings and several sites with formal positive or negative charges.[7b,c] Solvation around such large solutes necessarily reflects an average of the environment sampled by the solute, thus claims about the length scales over which solvation forces change are limited to the minimum distances of ∼1.5 nm (or ∼5 water layers) spanned by the solute. The smallest probe (*N*,*N*-diethyl-*p*-nitroaniline (DEPNA)) was used in nonlinear optical measurements characterizing solvent polarity at the air−aqueous and several organic−aqueous interfaces.[7a] While the optically active part of the DEPNA chromophore is similar in size to the organic solvents used, experiments were sensitive only to the equilibrium distributions and orientations of solutes at the different interfaces.[9] Missing was information about *how* the interfacial properties converged from aqueous to a nonpolar, organic limit. To understand the origins and extent of interfacial solvation, experiments must be able to discern how chemical solvation around a solute varies as the solute changes its equilibrium position relative to a nominal interfacial plane.

These considerations highlight the need to profile accurately solvation *across* different aqueous−organic, liquid−liquid boundaries as well as the interfaces formed between different solids and liquids. Accomplishing this goal requires tools that measure interfacial width. Described below are the methods used to create a homologous series of surfactants capable of probing changes in solvent environment on molecular length scales. These "molecular rulers" consist of hydrophobic, solvent-sensitive chromophores attached to polar or charged headgroups by means of simple, variable-length alkyl spacers. At liquid surfaces, molecular rulers form monolayers that span the interfacial region (Figure 1). The solvent-sensitive chromophore response provides a means of observing how the local solvation environment changes as a function of chromophore−headgroup separation. Implicit in this admittedly simple, schematic model is that the charged headgroup remains solvated in the aqueous phase while the hydrophobic, solvent-sensitive chromophore "floats" into the organic phase. The "resolution" of these rulers is limited by the size of the hydrophobic chromophore—intentionally chosen to be as small as possible—and the minimum size by which the spacers can be varied—nominally a single CH_2 group or ∼2.5 Å. While these rulers cannot provide unambiguous information about how solvent properties and structure vary across an interface, the solvent-sensitive response of the ruler chromophore can identify how the local chemical environment surrounding a solute changes with the solute's equilibrium distribution relative to an interfacial boundary. Results from surface-specific, nonlinear optical experiments show that this approach to measuring interfacial width holds tremendous potential for clarifying how surfaces impact solvation and how far into a solvent surface mediated effects extend.

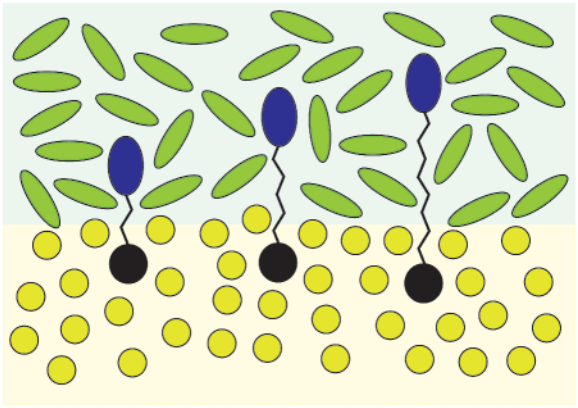

Figure 1. A schematic representation of molecular rulers adsorbed to a liquid−liquid interface.

Surfactants described below are but one example of a general strategy designed to measure changes in local environment on *molecular length scales*. The emphasis of this work is on the synthesis and characterization of a class of novel surfactants that can overcome the aforementioned limitations associated with experiments examining interfacial solvation. This approach of altering the equilibrium distribution of solutes across an interfacial boundary promises to provide quantitative information that can spur the development of more accurate solvation models. Molecular rulers may also find applications in environmentally and biologically important systems where knowledge about changes in chemical environment on sub-nanometer length scales is essential for formulating mechanisms of interfacial reactivity. Different applications may require using chromophores having different photophysical properties. Furthermore, molecular rulers can be constructed specifically for X-ray and neutron scattering experiments by incorporating

(8) (a) Benjamin, I.; Michael, D. *J. Phys. Chem. B* **1998**, *102*, 5145−5151. (b) Benjamin, I.; Squitieri, E. *J. Phys. Chem. B* **2001**, *105*, 6412−6419. (c) Benjamin, I.; Michael, D. *J. Chem. Phys.* **2001**, *114*, 2817−2822. (d) Pohorille, A.; Chipot, C.; Wilson, M. A. *J. Phys. Chem. B* **1997**, *101*, 782−791. (e) Pohorille, A.; Wilson, M. A. *J. Phys. Chem.* **1996**, *104*, 3760−3773. (f) Dang, L. X. *J. Phys. Chem. B* **2001**, *105*, 804−809. (g) Berkowitz, M.; Schweighofer, K. J.; Essmann, U. *J. Phys. Chem. B* **1997**, *101*, 3793−3799.

(9) Girault, H. H.; et al. *J. Chem. Soc., Faraday Trans.* **1996**, *92*, 3079−3085.

probes with sufficiently large scattering cross-sections at different positions within the ruler structure.

Criteria and Synthetic Overview

To profile solvation across different interfaces, molecular rulers must satisfy three criteria: (a) rulers must exhibit measurable sensitivity to changes in local solvation, (b) rulers must be surface active, and (c) rulers must be modular with simple synthetic methods for varying the separation between headgroup and chromophore.

Solvent Sensitivity. Solute solvatochromism can serve as a sensitive probe of local solvation environment.[10] Solvatochromism describes the solvent-sensitive shifts of a chromophore's transition energy and arises from the differential solvation of a solute's ground and excited states. If the chromophore's excited state dipole is larger than its ground state dipole, the excited state will be preferentially solvated, leading to a spectroscopically observable red-shift in the solute excitation spectrum relative to its gas-phase value. This red-shift becomes more pronounced with increasing solvent polarity.

Molecular rulers described in this work incorporate a derivative of *p*-nitroanisole (pNAs), a photoactive chromophore whose excitation wavelength red-shifts more than 20 nm as solvent polarity increases from that of cyclohexane to that of water.[11] The pNAs chromophore is ideal for use in molecular rulers because of its photochemical stability and its large change in permanent dipole upon excitation.[12] Furthermore, the small size of pNAs imparts finer spatial resolution to molecular rulers than would be afforded with large chromophores having extensive, delocalized electronic structures. Experiments profiling interfacial width will exploit these advantages by measuring effective excitation spectra of pNAs based molecular rulers adsorbed to different solid−liquid and liquid−liquid boundaries.

Surface Activity. The pairing of a hydrophobic probe and polar or ionic headgroup ensures that molecular rulers will be surface active. Surface activity is monitored by measuring the interfacial tension at liquid−liquid interfaces. The Gibbs isotherm for soluble monolayers provides a relationship between the excess surface concentration and the interfacial pressure:[13]

$$A\pi = A(\gamma_o - \gamma) = \Gamma kT \ln(c) \qquad (1)$$

Here, π is the interfacial pressure (the difference between the surface tensions of the neat interface (γ_o) and the system under study (γ)), A is the interfacial area, Γ is the surface excess concentration, k is Boltzmann's constant, T is temperature, and c is the bulk concentration of molecular ruler. At low bulk concentrations, the activity is assumed to be equivalent to concentration. Differentiating surface pressure with respect to ln(c) leads to the expression:

$$\frac{\partial \pi}{\partial \ln(c)} = \frac{\Gamma}{A} kT \qquad (2)$$

The limiting terminal surface concentration of the molecular ruler monolayers can be determined by plotting π vs ln(c) and determining the slope of steepest ascent.

Scheme 1. Molecular Ruler Synthesis[a]

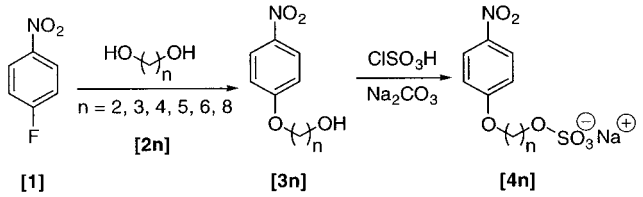

[a] In the text, rulers are assigned notations to distinguish their functionality (neutral alcohol, **3n**, or ionic sulfate, **4n**) and length. The lengths of the alkyl spacers present follow this scheme: **a** designates a two-carbon spacer, **b** a three-carbon spacer, **c** a four-carbon spacer, and so on. Thus, **3a** is the neutral alcohol containing a two-carbon spacer.

Experimental Section

Scheme 1 depicts the two-step synthesis used to create neutral and ionic molecular rulers. The starting material, *p*-nitrofluorobenzene (pNFB), is converted to the desired product **3n** by adding the 1,*n*-diol of desired length in the correct ratio to maximize the yield of the monomer.[14] After purification the alcohol is converted to an ionic salt upon reaction with chlorosulfonic acid according to published procedures.[15] Assuming an all-trans conformation, each methylene group increases the separation between the hydrophilic headgroup and hydrophobic chromophore by approximately 2.5 Å. This assumption is certain to break down with longer chains, but alkyl spacers up to five CH_2 groups in length should have either one or zero gauche defects.[16] The issue of alkyl chain conformation is discussed below in greater detail.

All reagents used were purchased from Aldrich and used without further purification. Diethyl ether was distilled from sodium/benzophenone ketyl. All reactions were run under an atmosphere of nitrogen. All compounds were >95% pure as determined by ^{1}H and ^{13}C NMR spectroscopy. Nuclear magnetic resonance (^{1}H and ^{13}C NMR) spectra were recorded on a 400 MHz spectrometer. Chemical shifts are reported in parts per million, relative to the nondeuterated solvent peak. Coupling constant (*J* values) are reported in hertz, and spin multiplicities are indicated by the following symbols: s (singlet), d (doublet), t (triplet), q (quartet), m (multiplet), br s (broad singlet). Infrared band positions are given in reciprocal centimeters (cm^{-1}) and relative intensities are listed as br (broad), s (strong), m (medium), or w (weak). Thin-layer chromatography (TLC) was performed with the compounds being identified in one or both of the following manners: UV (254 nm) and iodine.

General Procedure for the Synthesis of 3a−f. *p*-Nitrofluorobenzene (pNFB) was added dropwise to the mixture of diol and potassium hydroxide (KOH) at room temperature and stirred for 2 h. The reaction mixture was poured into water and extracted with diethyl ether. In addition to the desired product a 1,*n*-dimer and the residual starting material were also extracted into the ether. Purification of the reaction mixture residue by flash chromatography (hexanes:EtOAc, 3:2) gave the desired alcohol and starting material. The spectral data of the individual compounds are reported below.

2-(4-Nitrophenoxy)ethanol (3a). Compound **3a** was prepared by following the general procedure employing pNFB (0.998 g, 7.07 mmol), ethylene glycol (3.51 g, 56.5 mmol), and KOH (0.500 g, 8.91 mmol). Purification of the reaction mixture gave 0.215 g (22%) of pNFB and 0.694 g (54%) of **3a** as a white solid: mp 83−85 °C; R_f = 0.20 (hexanes:EtOAc, 3:2); IR (KBr) 3262 (s), 3106 (w), 2947 (w), 1503 (s), 1340 (s); ^{1}H NMR ($CDCl_3$) 2.02 (s, 1H), 4.01 (t, J = 4.4, 2H),

(10) Suppan, P.; Ghoneim, N. *Solvatochromism*; The Royal Society of Chemistry: Cambridge, UK, 1997; Chapter 2.
(11) Laurence, C.; et al. *J. Phys. Chem.* **1994**, *98*, 5807−5816.
(12) Whitaker, C. M.; McMahon, R. J.; et al. *J. Am. Chem. Soc.* **1996**, *118*, 9966−9973.
(13) Adamson, A. W. *Physical Chemistry of Surfaces*; John Wiley & Sons: New York, 1990; Chapter 2.
(14) Rarick, M.; Brewster, R.; Dains, F. *J. Am. Chem. Soc.* **1933**, *55*, 1289−1290.
(15) Lambrech, J. U.S. Patent 2,573,769, 1951.
(16) Strauss, H. L.; Snyder, R. G. *J. Phys. Chem.* **1982**, *86*, 5145−5150.

4.17 (t, $J = 4.4$, 2H), 6.98 (d, $J = 9.2$, 2H), 8.20 (d, $J = 9.2$, 2H); ^{13}C NMR ($CDCl_3$) 61.1, 70.0, 114.5, 125.9, 141.7, 163.6; LRMS (EI) 183 (M^+, 66), 139 (100); HRMS (EI) calcd for $C_8H_9O_4N$ 183.0532 (M^+), found 183.0536. See Supporting Information on pp S1−S4.

3-(4-Nitrophenoxy)propanol (3b). Compound **3b** was prepared by following the general procedure employing pNFB (0.998 g, 7.07 mmol), 1,3-propanediol (4.26 g, 56.0 mmol), and KOH (0.500 g, 8.91 mmol). Purification of the reaction mixture gave 0.335 g (34%) of pNFB and 0.715 g (51%) of **3b** as a yellow oil: $R_f = 0.25$ (hexanes:EtOAc, 3:2); IR (NaCl) 3358 (s), 3115 (w), 2952 (w), 1510 (s), 1265 (s); ^{1}H NMR ($CDCl_3$) 2.02 (dd, $J = 6.0$, 6.0, 2H), 2.33 (s, 1H), 3.80 (t, $J = 6.0$, 2H), 4.15 (t, $J = 6.0$, 2H), 6.89 (d, $J = 9.2$, 2H), 8.10 (d, 2H); ^{13}C NMR ($CDCl_3$) 31.6, 59.1, 65.7, 114.3, 125.8, 141.2, 163.9. LRMS (FAB) 198 ($(M + H)^+$, 100); HRMS (FAB) calcd for $C_9H_{12}O_4N$ 198.0766 $(M + H)^+$, found 198.0764. See Supporting Information on pp S5−S8.

4-(4-Nitrophenoxy)butanol (3c). Compound **3c** was prepared by following the general procedure employing pNFB (0.998 g, 7.07 mmol), 1,4-butanediol (3.19 g, 35.4 mmol), and KOH (0.500 g, 8.91 mmol). Purification of the reaction mixture gave 0.437 g (44%) of pNFB and 0.621 g (44%) of **3c** as a white solid: mp 78−80 °C; $R_f = 0.26$ (hexanes:EtOAc, 3:2); IR (KBr) 3527 (s), 3115 (w), 2954 (w), 1508 (s), 1262, (s); ^{1}H NMR ($CDCl_3$) 1.45 (s, 1H), 1.75 (q, $J = 6.2$, 2H), 1.91 (q, $J = 6.2$, 2H), 3.72 (t, $J = 6.2$, 2H), 4.08 (t, $J = 6.2$, 2H), 6.92 (d, $J = 9.2$, 2H), 8.17 (d, $J = 9.2$, 2H); ^{13}C NMR ($CDCl_3$) 25.5, 29.1, 62.4, 68.6, 114.4, 125.9, 141.4, 164.0; LRMS (FAB) 212 ($(M + H)^+$, 100), 140 (67); HRMS (FAB) calcd for $C_{10}H_{14}O_4N$ 212.0923 $(M + H)^+$, found 212.0928. See Supporting Information on pp S9−S12.

5-(4-Nitrophenoxy)pentanol (3d). Compound **3d** was prepared by following the general procedure employing pNFB (2.00 g, 14.1 mmol), 1,5-pentanediol (8.78 g, 84.3 mmol), and KOH (1.03 g, 18.3 mmol). Purification of the reaction mixture gave 0.363 g (18%) of pNFB and 2.09 g (66%) of **3d** as a yellow oil: $R_f = 0.20$ (hexanes:EtOAc, 3:2); IR (NaCl) 3361 (s), 3111 (w), 2940 (w), 1511 (s), 1265 (s); ^{1}H NMR ($CDCl_3$) 1.27 (t, $J = 6.0$, 1H), 1.50−1.60 (m, 2H), 1.60−1.65 (m, 2H), 1.80−1.90 (m, 2H), 3.68 (q, $J = 6.0$, 2H), 4.05 (t, $J = 6.4$, 2H), 6.92 (d, $J = 9.2$, 2H), 8.27 (d, $J = 9.2$, 2H); ^{13}C NMR ($CDCl_3$) 22.2, 28.7, 32.2, 62.6, 68.6, 114.3, 125.9, 141.3, 164.1. LRMS (FAB) 226 ($(M + H)^+$, 100), 69 (77); HRMS (FAB) calcd for $C_{11}H_{16}O_4N$ 226.1079 $(M + H)^+$, found 226.1085. See Supporting Information on pp S13−S16.

6-(4-Nitrophenoxy)hexanol (3e). Compound **3e** was prepared by following the general procedure employing pNFB (2.00 g, 14.1 mmol), 1,6-hexanediol (8.30 g, 70.2 mmol), and KOH (1.03 g, 18.3 mmol) at 50−60 °C. Purification of the reaction mixture gave 0.321 g (16%) of pNFB and 0.213 g (63%) of **3e** as a white solid: mp 80−83 °C; $R_f =$ 0.31 (hexanes:EtOAc, 3:2); IR (KBr) 3516 (s), 3115 (w), 2930 (w), 1500 (s), 1258 (s); ^{1}H NMR ($CDCl_3$) 1.28 (s, 1H), 1.40−1.65 (m, 6H), 1.80−1.85 (m, 2H), 3.65 (s, 2H), 4.03 (t, $J = 6.4$, 2H), 6.91 (d, $J =$ 9.2, 2H), 8.17 (d, $J = 9.2$, 2H); ^{13}C NMR ($CDCl_3$) 25.5, 25.7, 28.9, 32.6, 62.8, 68.7, 114.4, 125.9, 141.3, 164.1; LRMS (FAB) 240 ($(M + H)^+$, 99), 55 (100); HRMS (FAB) calcd for $C_{12}H_{18}O_4N$ 240.1236 $(M + H)^+$, found 240.1233. See Supporting Information on pp S17−S20.

8-(4-Nitrophenoxy)octanol (3f). Compound **3f** was prepared by following the general procedure employing pNFB (0.998 g, 7.07 mmol), 1,8-octanediol (6.20 g, 42.4 mmol), and KOH (0.500 g, 8.91 mmol) at 50−60 °C. Purification of the reaction mixture gave 0.345 g (35%) of pNFB and 0.923 g (49%) of **3f** as a white solid: mp 86−88 °C; $R_f =$ 0.35 (hexanes:EtOAc, 3:2); IR (KBr) 3516 (s), 3111 (w), 2929 (w), 1499 (s), 1260 (s); ^{1}H NMR ($CDCl_3$) 1.24 (t, $J = 5.6$, 1H), 1.30−1.60 (m, 10H), 1.75−1.85 (m, 2H), 3.63 (q, $J = 5.6$, 2H), 4.02 (t, $J = 6.4$, 2H), 6.91 (d, $J = 9.2$, 2H), 8.17 (d, $J = 9.2$, 2H); ^{13}C NMR ($CDCl_3$) 25.6, 25.8, 28.9, 29.2, 29.3, 32.7, 63.0, 68.8, 114.4, 125.9, 141.3, 164.2; LRMS (FAB) 268 ($(M + H)^+$, 56), 69 (100); HRMS (FAB) calcd for $C_{14}H_{22}O_4N$ 268.1549 $(M + H)^+$, found 268.1546. See Supporting Information on pp S21−S24.

General Procedure for the Synthesis of 4a−e. Chlorosulfonic acid was added to the solution of the corresponding alcohol in diethyl ether at room temperature and stirred for 1 h. A 10% sodium carbonate solution was added until the pH rose to 10. The water and any remaining ether were then removed by rotary evaporation. The product was separated from the mixture of solids with several acetonitrile extractions. Evaporating the acetonitrile left solely the product of interest as a sodium salt. The spectral data of the individual compounds are reported below.

Sodium 2-(4-Nitrophenoxy)ethyl Sulfate (4a). Compound **4a** was prepared following the general procedure employing chlorosulfonic acid (0.390 g, 3.35 mmol) and compound **3a** (0.471 g, 2.57 mmol). Evaporating the acetonitrile gave 0.618 g (82%) of **4a** as an off-white solid: IR (KBr) 3517 (s), 3254 (s), 3115 (w), 1494 (s), 1250 (m); ^{1}H NMR (D_2O) 4.22 (s, 4H), 6.90 (d, $J = 9.2$, 2H), 8.00 (d, $J = 9.2$, 2H); ^{13}C NMR (D_2O) 66.8, 67.0, 114.9, 126.1, 141.2, 163.6. See Supporting Information on pp S25−S29.

Sodium 4-(4-Nitrophenoxy)butyl Sulfate (4c). Compound **4c** was prepared following the general procedure employing chlorosulfonic acid (3.12 g, 26.8 mmol) and compound **3c** (2.26 g, 10.7 mmol). Evaporating the acetonitrile gave 2.67 g (80%) of **4c** as a white solid: IR (KBr) 3498 (s), 3113 (w), 1501 (s), 1263 (m); ^{1}H NMR (D_2O) 1.65−1.71 (m, 4H), 3.95 (t, $J = 5.6$, 4H), 6.82 (d, $J = 9.2$, 2H), 7.95 (d, $J = 9.2$, 2H); ^{13}C NMR (D_2O) 24.7, 25.1, 68.5, 68.9, 114.7, 126.1, 140.8, 164.1. See Supporting Information on pp S30−S34.

Sodium 6-(4-Nitrophenoxy)hexyl Sulfate (4e). Compound **4e** was prepared following the general procedure employing chlorosulfonic acid (1.30 g, 11.2 mmol) and compound **3e** (1.34 g, 5.58 mmol). Evaporating the acetonitrile gave 1.53 g (81%) of **4e** as an off-white solid: IR (KBr) 3479 (s), 3117 (w), 1508 (s), 1259 (s); ^{1}H NMR (D_2O) 1.10−1.15 (s, 4H), 1.40−1.45 (m, 4H), 3.70−3.85 (m, 4H), 6.62 (d, $J = 8.4$, 2H), 7.77 (d, $J = 8.4$, 2H); ^{13}C NMR (D_2O) 24.8, 24.9, 28.2, 28.5, 69.0, 69.2, 114.5, 125.8, 140.5, 164.2. See Supporting Information on pp S35−S39.

The neutral alcohol species **3a**−**f** serve as excellent probes of hydrophilic solid−liquid interfaces. The alcohol functional group can hydrogen bond with silanol-terminated quartz surfaces allowing the chromophore to probe local solvation environments different distances away from the solid−liquid boundary. Surface-specific nonlinear optical measurements described elsewhere show how different length rulers sample regions of significantly different polarities, despite the fact that the bulk dielectric properties of the solvents being studied can be quite similar.[17] In addition, preliminary studies have shown that the ionic species **4a**−**e** are also successful as probes of weakly interacting liquid−liquid interfaces. Data comparing results from the shortest ruler with those from the parent pNAs chromophore are discussed below.

One unusual aspect of the characterization warrants mention here. Fast atom bombardment (FAB) mass spectrometry provides unambiguous identification of the neutral alcohol species (**3a**−**f**). The ionic sulfates, however, need to be identified by using electrospray mass spectrometry. Mass spectra of species **4a**, **4c**, and **4e** recorded using anion detection show dominant features corresponding to the monomer anion (r^-) mass (Figure 2). Careful inspection of the spectra show small, additional features at higher masses corresponding to $[r_2Na_1]^-$ up to hexamer clusters ($[r_6Na_5]^-$). These aggregates provide evidence that samples are, in fact, the sodium salt. Except for species **4a**, these larger clusters have very small intensities relative to that of the parent monomer anion. In the **4a** anion spectrum, the dimer $[r_2Na_1]^-$ has ∼50% of the intensity of the monomer anion.

Spectral patterns change dramatically in the positive ion spectra. Data for **4a**, **4c**, and **4e** show long progressions out to the detection limits of the instrument (2000 amu, see Figure 3). These progressions correspond to aggregates of anion:sodium complex with an additional sodium ion $[r_nNa_{n+1}]^+$. The progression extends out to the hexamer

(17) Steel, W. H.; Zhang, X.; Walker, R. A. In preparation.

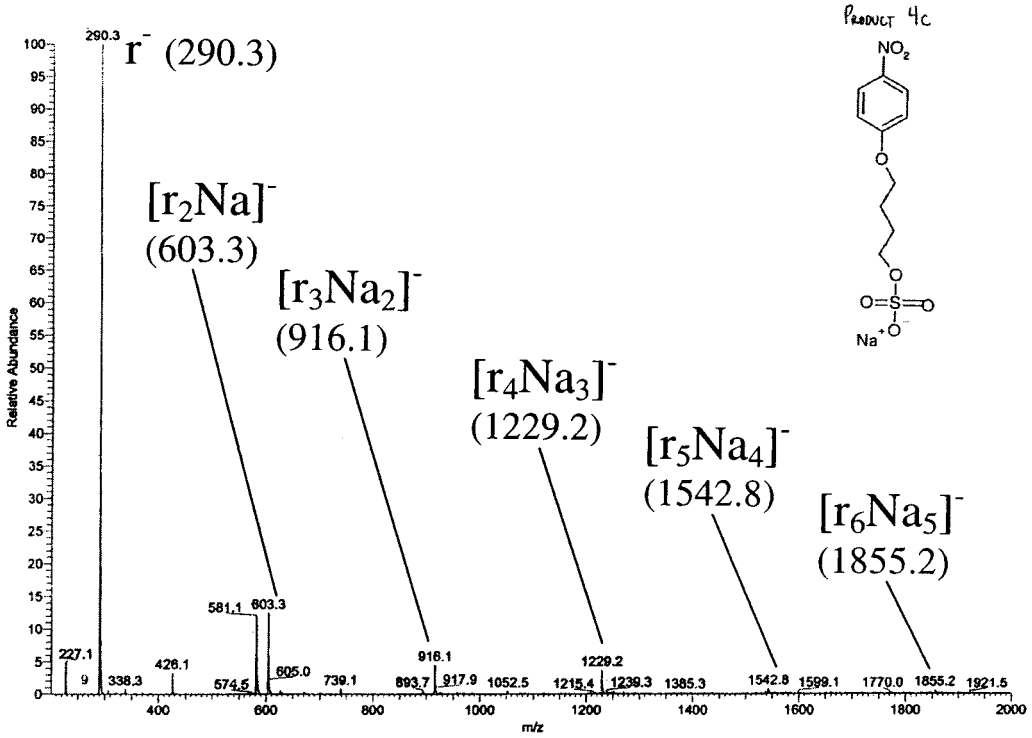

Figure 2. Negative ion electrospray mass spectrum of **4c**. The ruler anion [r] appears as the dominant feature (*m*/*z* 290 amu). Aggregates $[r_nNa_{n-1}]^-$ are labeled out to the hexamer. In contrast to the positive ion spectrum, intensity in the larger aggregates drops off dramatically above the dimer, $[r_2Na_1]^-$. Negative ion spectra of **4a** and **4e** can be found in the Supporting Information.

($[r_6Na_7]^+$) with appreciable intensity. Analysis of each band indicates that the primary component is the multimer in a +1 charge state. While the mechanism of charged aggregate formation remains unclear,[18] the gas-phase ions are generated from small, highly charged droplets in which the effective solute concentration has increased ~100-fold.[19] Droplets that contain excess cation or anions form the charged clusters detected by the spectrometer. The more pronounced progressions in the cation spectra likely reflect the preferred solvation energetics associated with small cations (Na^+) compared to bulkier anions ($R-SO_4^-$).[19] In other words, droplets containing *n* ruler anions and (*n* + 1) Na^+ cations are thermodynamically more stable (and prevalent) than stoichiometries leading to corresponding anionic aggregates. Similar phenomena have been observed in solutions of simple surfactants as well as numerous inorganic salts.[18,19]

Characterization

Solvatochromic Behavior. Figure 4 displays the solvatochromic behavior of **3a**, **3d**, **3f**, and pNAs. Shown are excitation maxima plotted against the polarity function for a representative sample of protic and aprotic solvents. The polarity function, *f*(*D*), is directly related to the solvent dielectric constant:

$$f(D) = \frac{2(\epsilon - 1)}{2\epsilon + 1} \qquad (3)$$

where ϵ is the solvent's static dielectric constant. Typical *f*(*D*) values for common solvents range from ~0.4 (alkanes) to ~1 (water). A linear relationship between *f*(*D*) and solute excitation maxima typically indicates solute sensitivity to long-range, nonspecific solvation forces.[10,20]

The solvatochromic behavior of all alcohol species is quite similar to that of the original pNAs chromophore. Data show a linear relationship across a wide range of solvents—both protic and aprotic—with the only significant deviation appearing in aqueous solution. Furthermore, excitation spectra of the different salts (**4a**, **4c**, and **4e**) in aqueous solution are identical with spectra from the corresponding alcohols, indicating that the second step in Scheme 1 leaves the electronic structure of the chromophore unchanged. Consequently, ruler excitation energies provide a sensitive measure of local solvation environments in interfacial systems.

Surface Activity. The Wilhelmy Plate method[13] was used to measure the surface activity of different rulers at an aqueous–cyclohexane interface. Figure 5 shows the surface pressure isotherms of products **4a**, **4c**, and **4e**. Fitting the data according to eqs 1 and 2 shows the terminal surface concentrations of species **4a**, **4c**, and **4e** to be 1.49×10^{14}, 1.66×10^{14}, and 1.89×10^{14} molecules/cm^2, respectively. These results compare favorably to surface concentrations for other alkyl surfactants at weakly associating liquid–liquid interfaces.[21] An interesting observation is that the terminal surface concentration appears to increase slightly with increasing alkyl chain length, consistent with the idea that more hydrophobic species should exhibit greater surface activity. The well-behaved surface activity exhibited in Figure 5 enables experiments examining interfacial solvation to be carried out with well-defined ruler surface concentrations up to the reported terminal concentrations.

At aqueous–organic interfaces, rulers form anionic monolayers with surfactant separation being controlled by Coulomb repulsions between individual headgroups. Reported surface excess concentrations correspond to areas of ~50–70 Å^2/

(18) Hao, C.; March, R. E. *J. Mass Spectom.* **2001**, *36*, 509–521.
(19) Siuzdak, G.; Bothner, B. *Angew. Chem., Int. Ed. Engl.* **1995**, *34*, 2053–2055.
(20) Wong, M. W.; Frisch, M. J.; Weiberg, K. B. *J. Am. Chem. Soc.* **1991**, *113*, 4776–4782.
(21) Watry, M. R.; Richmond, G. L. *J. Am. Chem. Soc.* **2000**, *122*, 875–883.

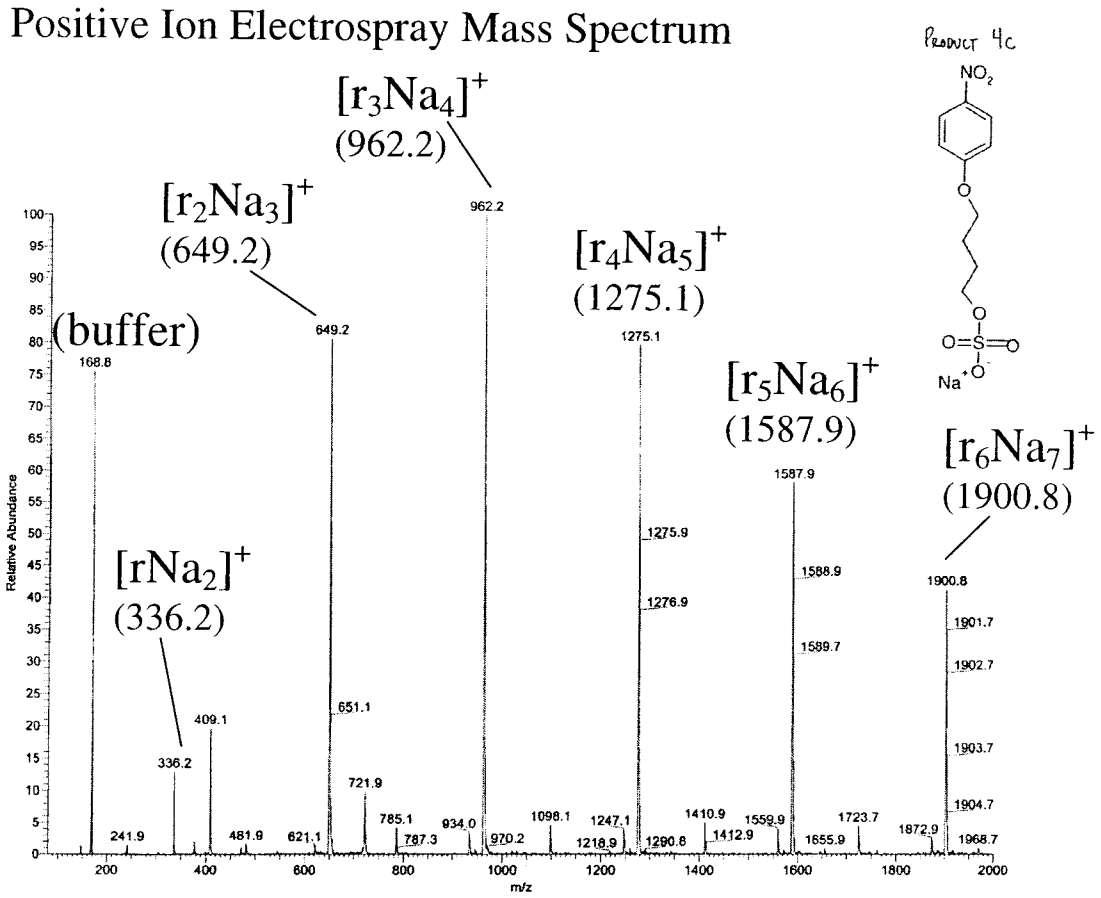

Figure 3. Positive ion electrospray mass spectrum of **4c**. The feature at 168 amu arises from the buffer used to dissolve the molecular ruler. Aggregates $[r_nNa_{n+1}]^+$ are labeled out to the hexamer. Isotopic separation of equivalently sized aggregates indicate that species are predominantly in the +1 charge state. Positive ion spectra of **4a** and **4e** can be found in the Supporting Information.

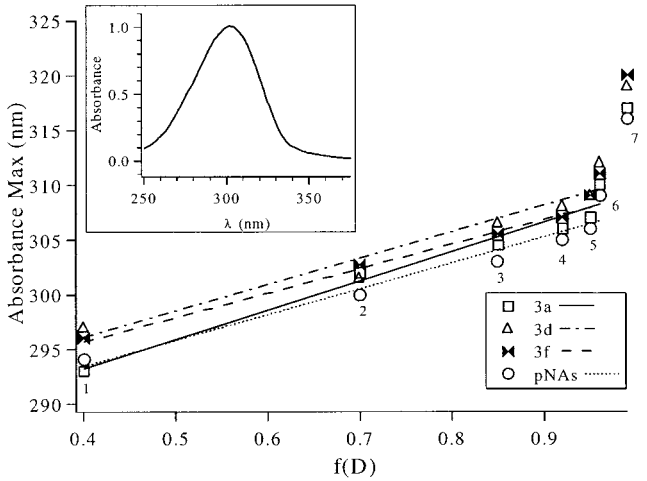

Figure 4. Solvatochromic behavior of products **3a**, **3d**, and **3f**, with comparison to pNAs. Data demonstrate that the alcohol species retain the solvatochromic characteristics of pNAs. UV maxima were recorded in (1) cyclohexane, (2) diethyl ether, (3) 1-octanol, (4) ethanol, (5) methanol, (6) acetonitrile, and (7) water. The inset shows a representative UV spectrum, recorded for product **3d** in 1-octanol.

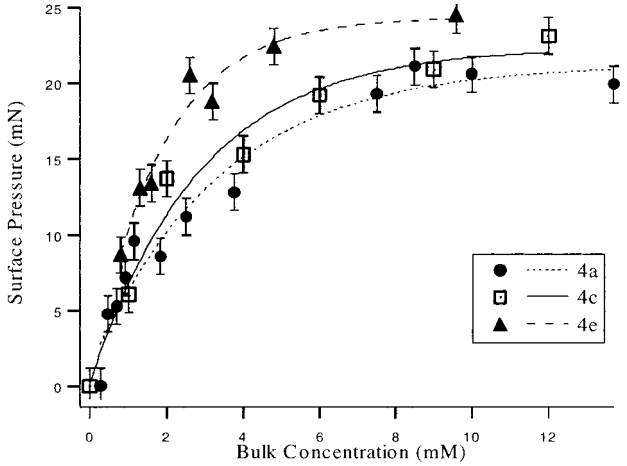

Figure 5. Interfacial pressure isotherms for representative molecular ruler salts at an aqueous−cyclohexane boundary. Data were fit with Langmuir isotherms which in turn were used to calculate terminal surface concentrations of products **4a**, **4c**, and **4e**.

molecule. This figure represents approximately three times the area occupied by *neutral* surfactants packed to their hard sphere limits (e.g. long-chain carboxylic acids).[9] The fact that these pNAs-based surfactants do not form tightly packed monolayers raises several concerns about their ability to function as molecular rulers. Issues of spacer conformation and surfactant aggregation are addressed below.

First, relatively low surface concentrations (compared to the tightly packed, hard sphere limit) enable the alkyl spacers to adopt multiple conformations. Gauche defects in the alkyl chain will shorten the effective length of the molecular ruler and, consequently, the ruler's ability to distinguish changes in solvation across different liquid−liquid interfaces. Obviously,

multiple conformations and reduced ruler effectiveness become concerns as alkyl spacers get longer. However, Raman and X-ray scattering studies of alkanes in solution show that >90% of linear alkanes up to 5 C atoms in length exist in conformations that are either all-trans or incorporate a single gauche defect.[16,22] Furthermore, nonlinear optical studies of alkyl chain structure in monolayers adsorbed to liquid−liquid interfaces show that short-chain surfactants exhibit fewer gauche defects than long-chain alkyl surfactants.[23] Molecular dynamics simulations suggest that the greatest propensity for gauche defects in surfactants adsorbed to liquid surfaces exists in the second C−C bond after the charged headgroup. The order parameter for alkyl chains then remains constant through 6 CH_2 groups.[8g] Interestingly, charged surfactant monolayers exhibit less conformational order at air−water interfaces than at liquid−liquid interfaces, a result that stands in contrast to results from neutral monolayers that can achieve higher surface concentrations.

Given the short lengths of the alkyl spacers used in the molecular rulers described above *and* the surface-induced polar ordering at liquid−liquid interfaces, we anticipate that conformational disorder within adsorbed surfactants will not hamper their ability to sample changes in solvation across liquid−liquid interfaces. An empirical method for assessing conformational order within alkyl chains involves comparing relative intensities of different CH_2 infrared vibrational bands.[16] One such pair of bands are those assigned to the CH_2 symmetric stretch (at ∼2850 cm^{-1}) and the CH_2 antisymmetric stretch/Fermi resonance (at 2930 cm^{-1}). The I_{2850}/I_{2930} ratio varies from less than 1.0 in well-ordered systems of *n*-alkanes to a limiting value of ∼3 for long, *n*-alkyl chains (e.g. $>C_{22}$) having statistical distributions of gauche defects.[16] Fits to IR spectra of **3e** dissolved in CCl_4 yield a I_{2850}/I_{2930} ratio of 0.7(±0.1) (data not shown). This result is further evidence that spacer flexibility should not diminish the ability of these molecular ruler surfactants to span different interfacial widths. Systems requiring rulers with longer spacers (>6 carbons) will need additional characterization by surface-specific, NLO vibrational spectroscopy to ascertain chain conformation. Alternatively, rulers can be created with rigid, nonconjugated spacers such as fused norbornane ring systems.[24]

The effect(s) of surfactant aggregation on the photophysical properties of the hydrophobic chromophore represents a second source of concern about the surfactants' abilities to function as molecular rulers. Aggregation-induced quenching or energy transfer between chromophores will not be important due to the reasonably large separation between chromophores (∼1 nm chromophore−chromophore separation at full monolayer coverage), the narrow bandwidth of the excitation and emission bands, and the large difference in energy between chromophore absorption and emission.

Furthermore, the probe of interfacial solvation—resonant second harmonic generation—does not result in chromophore excitation (*vide infra*). Of greater concern is the effect of soluble monolayer formation from anionic headgroup−cationic counterion pairing. The presence of charged species so close to the pNAs chromophore could lead to anomalously large electric fields inside of the solute cavity. If double-layer formation influences probe solvation, we would expect the data to reflect large solvatochromic shifts, consistent with the effects of electric fields measuring 10^7 V/cm. In fact, NLO data for the shortest of the molecular rulers (**4a**) show that the ruler probe samples a *less polar* environment than the neutral parent, pNAs chromophore. This observation supports the picture of the hydrophobic ruler chromophore interacting strongly with the organic phase, effectively screened from field effects arising from the charged headgroup and counterion interactions.[25]

Nonlinear Optical Spectroscopy. Second harmonic generation (SHG) is a nonlinear optical method that can measure effective excitation spectra of species at interfaces.[1b,c] Due to its origins, SHG is both surface and molecularly specific, meaning that spectra result only from solutes that experience interfacial anisotropy.[2b,d,e] In a typical SHG experiment, a single coherent optical field with frequency ω is focused on the interface under study, and a nonlinear polarization with frequency 2ω is detected. The intensity of the 2ω field is proportional to the square of the second-order susceptibility, $\chi^{(2)}$

$$I(2\omega) \propto |\chi^{(2)}|^2 I(\omega)^2 \tag{4}$$

where $I(\omega)$ is the intensity of the incident field and $\chi^{(2)}$ is a third rank tensor that under the electric dipole approximation is zero in isotropic environments. The $\chi^{(2)}$ tensor is responsible for the technique's inherent surface specificity, and contains both nonresonant and resonant contributions:

$$\chi^{(2)} = \chi_{NR}{}^{(2)} + \chi_R{}^{(2)} \tag{5}$$

Typically, the resonant term is several orders of magnitude larger than the nonresonant contribution and can be related to microscopic hyperpolarizability:

$$\chi_R{}^{(2)} = \sum_{k,e} \frac{\mu_{gk}\mu_{ke}\mu_{eg}}{(\omega_{gk} - \omega - i\Gamma)(\omega_{eg} - 2\omega + i\Gamma)} \tag{6}$$

where $\mu_{i,j}$ is the transition matrix element between state i and state j (where g stands for ground state, k for an intermediate, virtual state, and e for the first excited state). When 2ω is resonant with ω_{eg}, $\chi^{(2)}$ becomes large leading to a strong resonance enhancement in the observed intensity at 2ω. Thus, measuring the scaled intensity $[I(2\omega)/I^2(\omega)]$ as a function of 2ω records an *effective* excitation spectrum of solutes adsorbed to an interface.

Figure 6 shows the SHG spectra of pNAs and **4a** adsorbed to an aqueous−cyclohexane interface. Also shown are the excitation maxima for pNAs in both solvents. In aqueous solution, λ_{max} values for pNAs, **3a**, and **4a** differ by less than 2 nm, while pNAs and **3a** share similar excitation wavelengths in cyclohexane. Cyclohexane's low dielectric constant prevents **4a** from dissolving in the organic phase. The pNAs spectrum appears in the bottom panel and shows a single, sharp feature. Fitting the data with eqs 4−6 (including the nonresonant contribution to $\chi^{(2)}$) leads to a transition wavelength maximum of 309 ± 2 nm. This result is consistent with aforementioned models that report interfacial polarity at liquid−liquid interfaces to represent an arithmetic mean of contributions from the two adjacent solvents.[2b,3] Although noisy, the **4a** spectrum shows

(22) Habenschuss, A.; Narten, A. H. *J. Chem. Phys.* **1990**, *92*, 5692−5699.
(23) (a) Walker, R. A.; Richmond, G. L.; Gruetzmacher, J. A. *J. Am. Chem. Soc.* **1998**, *120*, 6991−7003. (b) Conboy, J. C.; Richmond, G. L.; Messmer, M. C. *Langmuir* **1998**, *14*, 6722−6727.
(24) Paddon-Row: M. N.; et al. *J. Am. Chem. Soc.* **1987**, *109*, 3258−3269.
(25) Pratt, L. R. *J. Phys. Chem.* **1992**, *96*, 25−33.

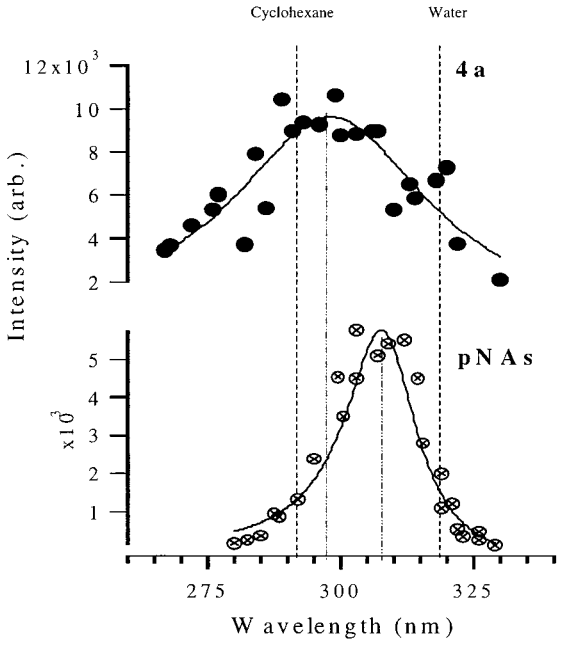

Figure 6. Second Harmonic generation spectra of product **4a** and pNAs at an aqueous−cyclohexane interface. The figure also shows the absorption maxima of **4a** in both bulk cyclohexane and water (dashed lines). Solid lines represent fits of data to eqs 4−6.

that the ruler chromophore also samples an interfacial polarity intermediate between that of cyclohexane and that of water. The data, however, are weighted toward the cyclohexane limit with a calculated transition wavelength maximum of 300 ± 4 nm. This large wavelength disparity between the pNAs and **4a** spectra implies that the chromophore of **4a** samples an environment that is significantly less polar than that sampled by pNAs, consistent with the idea that **4a** spans the aqueous−cyclohexane interface leaving the ruler chromophore more strongly solvated by the organic solvent.

The data in Figure 6 provide additional evidence that surfactant aggregation is not significantly influencing ruler chromophore solvation. Strong fields such as those found within double layers strongly enhance a molecule's hyperpolarizability leading to a large enhancement in the second harmonic response. While experimental limitations prevent quantitative absolute intensity comparisons between the **4a** and bare pNAs data, the normalized signal levels of the two spectra differ by approximately a factor of 2, rather than the order of magnitude enhancement that typically results from electric field induced second harmonic generation.[26] The difference in normalized signal levels can easily be accounted for by the difference between the surface concentrations of ruler **4a** and pNAs, 1.5 × 10^{14} and 0.5 × 10^{14}, respectively. Furthermore, we would expect any ion related field effects to shift chromophore excitation to longer wavelengths, consistent with the solvatochromic behavior observed in Figure 4. In fact, the spectrum of ruler **4a** shifts almost 10 nm to *shorter wavelengths*, consistent with the idea that the **4a** chromophore samples a less polar environment than the simple, bare pNAs probe adsorbed to the aqueous−cyclohexane interface. That the adsorbed chromophore shows any resonant signal at all implies that ruler **4a** is still influenced by surface-induced anisotropy. In the limit that the chromophore samples a bulklike, isotropic environment, the $\chi^{(2)}$ tensor would be zero by symmetry and a SHG experiment would show no wavelength-dependent, resonant response. If applicable, anisotropy resulting from chromophore−chromophore interactions will enhance the $\chi^{(2)}$ tensor by only ∼15% over a monolayer concentration of (0.5−1.5) × 10^{14} molecules/cm^2.[27] High chromophore density, however, would again create larger fields around solutes leading to a more polar environment, not less polar. Keeping these effects in mind, we can say that the 5 Å separation between headgroup and chromophore in **4a** represents an upper limit to the effective width of the aqueous−cyclohexane interface. Additional experiments probing the influence of organic solvent identity, monolayer concentrations, and temperature are ongoing.

Conclusions

We have synthesized series of neutral and ionic surfactants consisting of hydrophobic chromophores connected to hydrophilic headgroups by *n*-alkyl spacers. Neutral and ionic rulers can be produced with moderate yields and high purity. The solvatochromic behavior of all surfactants closely mimics that of the parent, *p*-nitroanisole chromophore. The solvent-sensitive chromophore and a variable separation between the chromophore and headgroup raises the possibility that these surfactants can be used to measure changes in noncovalent forces across interfaces on molecular length scales, thus overcoming a number of challenges faced by previous studies of interfacial solvation. Specifically, changing the length of the *n*-alkyl spacer should, in principle, change the equilibrium distribution of chromophores relative to a nominal interfacial boundary. Preliminary surface-specific, nonlinear optical experiments with the shortest ionic surfactant and the bare, parent pNAs chromophore indicate that the surfactants do, in fact, function as molecular rulers. Separating the pNAs-based probe from the charged, sulfate headgroup by only two methylene groups (∼5 Å) shifts the effective excitation spectrum at the aqueous−cyclohexane interface by almost 10 nm to shorter wavelengths relative to the bare chromophore spectrum. This observation is consistent with a model that allows the surfactant chromophore to "float" into the organic phase and sample a less polar environment. Furthermore, these results support recent models of interfacial solvation that predict aqueous−alkane liquid−liquid boundaries to be molecularly sharp and microscopically flat. On the basis of the generality of the synthesis and characterization of these surfactants, as well as the promise from initial nonlinear optical studies, we anticipate that molecular rulers will be powerful tools that can profile solvation across a wide variety of environmentally and biologically relevant interfaces.

Acknowledgment. The authors gratefully acknowledge support from the Research Corporation (RI0362) and equipment donations from Clark-MXR. R.N. acknowledges support from the National Science Foundation (NSF-MRSEC, DMR-0080008). We thank Jeff Davis, Jason Lagona, and Chris Handy for helpful discussions and N. Whitaker (N.I.H.) for mass spectrometric assistance.

Supporting Information Available: Spectra (PDF). This material is available free of charge via the Internet at http://pubs.acs.org.

JA012457U

(26) (a) Gragson, D. E.; Richmond, G. L. *J. Am. Chem. Soc.* **1998**, *120*, 366−375. (b) Whitaker, C. M.; McMahon, R. J.; et al. *J. Am. Chem. Soc.* **1996**, *118*, 9966−9973.
(27) Xu, Z.; Dong, Y. *Surf. Sci.* **2000**, *445*, L65-L70.